Directed evolution of D-2-keto-3-deoxy-6-phosphogluconate aldolase to new variants for the efficient synthesis of D- and L-sugars

Sun Fong, Timothy D Machajewski, Chi Ching Mak and Chi-Huey Wong

Background: Exploitation and improvement of enzymes as catalysts for organic synthesis is of current interest in biocatalysis. A representative enzyme for investigation is the *Escherichia coli* D-2-keto-3-deoxy-6-phosphogluconate (KDPG) aldolase, which catalyzes the highly specific reversible aldol reaction using the D-configurated KDPG as substrate.

Results: Using in vitro evolution, the aldolase has been converted into aldolases with improved catalytic efficiency, altered substrate specificity and stereoselectivity. In particular, some evolved aldolases capable of accepting both D- and L- glyceraldehyde in the non-phosphorylated form as substrates for reversible aldol reaction have been obtained, providing a new direction to the enzymatic synthesis of both D- and L-sugars.

Conclusions: This research has demonstrated the effectiveness of using in vitro evolution to rapidly alter the properties of an aldolase to improve its utility in asymmetric synthesis. The evolved aldolases, differing from the native enzyme which is highly phosphate- and D-sugar-dependent, catalyze the efficient synthesis of both D- and L-sugars from non-phosphorylated aldehydes and pyruvate. The principles and strategies described in this study should be applicable to other aldolases to further expand the scope of their synthetic utility.

Department of Chemistry and the Skaggs Institute for Chemical Biology, The Scripps Research Institute, 10550 North Torrey Pines Road, La Jolla, CA 92037, USA

Correspondence: Chi-Huey Wong
E-mail: wong@scripps.edu

Keywords: Aldolase; Directed evolution; D- and L-Sugars; *Escherichia coli*

Received: **18 May 2000**
Revisions requested: **27 July 2000**
Revisions received: **8 September 2000**
Accepted: **8 September 2000**

Published: **22 September 2000**

Chemistry & Biology 2000, **7**:873–883

1074-5521/00/$ – see front matter

PII: S1074-5521(00)00035-1

Introduction

As part of our interest in developing new enzymatic aldol reactions for organic synthesis [1], we report here the use of directed evolution to alter the D-sugar- and phosphate-dependent *Escherichia coli* D-2-keto-3-deoxy-6-phosphogluconate (KDPG) aldolase to new variants capable of making D- and L-sugars from pyruvate and non-phosphorylated aldehyde substrates (Figure 1).

A primary goal of protein engineering is to generate proteins with new or improved properties as a means to complement the shortcomings of known natural enzymes. Directed or in vitro evolution has recently been explored as a more generally applicable approach than the traditional rational methods towards the modification of enzyme properties [2]. The approach has the key advantage that a priori knowledge about the relationship between molecular architecture and function is not required for experimental design.

It has been demonstrated that in vitro evolution can yield new enzymes with altered substrate specificity [3–6] and topology [7], enantioselectivity [8,9], thermal stability [10,11], and organic solvent resistance [12,13]. A variety of studies that differ in the mutagenesis method and frequency, the size of library, and the use of screening or selection have been reported. However, which evolution strategy is most effective and whether a given protein property can be readily evolved by applying a certain strategy is unclear. Nonetheless, most of the practical situations lack a suitable selection system and require mutant libraries to be screened under specific reaction condition, thereby limiting the size of population that can be sampled.

The KDPG aldolase chosen for this study is a synthetically useful catalyst for the stereo-controlled formation of carbon–carbon bonds [14]. It catalyzes the reversible addition of pyruvate to a number of aldehydes to form the 4-substituted-4-hydroxy-2-ketobutyrate products. The natural biological function of the enzyme is to catalyze the cleavage of KDPG, a key intermediate in the Entner–Doudoroff pathway of bacterial sugar acid metabolism [15]. The enzyme is specific for the open-chain form of KDPG, which exists at approximately 9% in aqueous solution at neutral pH. The enzyme appears to be highly optimized for the turnover of KDPG in the cleavage reaction, and D-glyceraldehyde-3-phosphate in the addition reaction [16]. In addition, the aldolase is highly specific for aldehyde substrates with the D-configuration at the C2 position in the addition reaction [14]. We sought to explore the feasibility of small-scale laboratory evolution to improve the catalytic properties of an enzyme, by screening only a small population (10^3) of libraries with low mutation rate (2–3 bases per 640 bases). Specifically, we are interested in obtaining

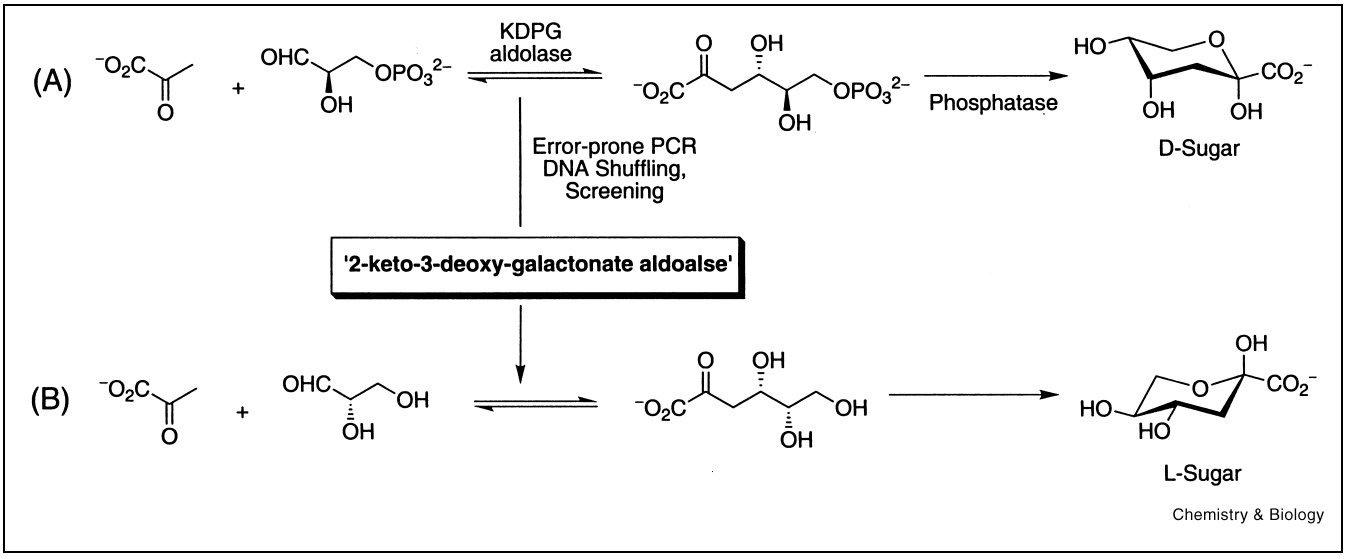

Figure 1. (A) The natural reaction catalyzed by native KDPG aldolase, followed by removal of the phosphate catalyzed by phosphatase. **(B)** One of the reactions that has been improved by mutagenesis and screening in this study.

variants of the aldolase that are more efficient in accepting non-phosphorylated substrates, as preparation of phosphorylated aldehydes is not trivial and most of the synthetically useful products are not phosphorylated. Hence, alteration of KDPG aldolase to accept non-phosphorylated substrates by successive mutation–screening cycles was attempted. In addition, we examined the possibility of altering the substrate enantioselectivity of the enzyme, by screening for mutants that accept L-glyceraldehyde, which was previously reported to be a non-substrate for the wild-type KDPG aldolase although we observed that the wild-type enzyme accepts the aldehyde poorly.

Results and discussion

Directed evolution of KDPG aldolase to new variants accepting the phosphate-free D-2-keto-3-deoxygluconate

Wild-type KDPG aldolase poorly accepts the non-phosphorylated substrate D-2-keto-3-deoxygluconate (KDG) compared with KDPG, with a 60-fold less favorable turnover and 800-fold less favorable apparent K_M (Table 1). The high K_M could be due to the fact that KDG exists mostly in cyclic pyranose and furanose forms whereas the enzyme is specific for the open-chain form of the phosphorylated substrate. We anticipated that an improvement in the efficiency of enzymatic KDG cleavage might also produce positive result for the enzyme's ability to catalyze reactions that involve other non-phosphorylated substrates. A screening approach based on KDG cleavage was then

Table 1
Kinetic parameters of KDPG aldolase variants for KDG and KDPG cleavage in 50 mM potassium phosphate, pH 7.5, containing 5 mM β-mercaptoethanol at 25°C.

Enzyme	Melting temperature	KDG cleavage			KDPG cleavage		
	(°C)[a]	K_M (mM)	k_{cat}/K_M (mM^{-1} s^{-1})	k_{cat} (s^{-1})	K_M (mM)	k_{cat}/K_M (mM^{-1} s^{-1})	k_{cat} (s^{-1})
Wild-type	58.1 (1.1)	284.9 (36)	0.016	4.6 (0.5)	0.35 (0.01)	811	283.8 (3.4)
KA1-4	–	54.7 (2.6)	0.11	6.0 (0.2)	–	–	–
KA1-3	60.3 (3.0)	48.7 (1.2)	0.13	6.1 (0.1)	0.21 (0.04)	516	108.3 (6)
KA1-2	60.7 (2.7)	25.0 (1.2)	0.16	4.1 (0.1)	0.15 (0.02)	619	92.8 (2.6)
KA1-1	–	64.8 (3.1)	0.10	6.6 (0.02)	–	–	–
KA2	66.3 (2.2)	14.3 (1.6)	0.58	8.3 (0.5)	0.03 (0.002)	1.71×10^3	51.5 (0.7)
KA3	59.2 (0.8)	12.8 (0.5)	1.09	13.9 (0.1)	0.03 (0.008)	93	2.5 (1.2)
KA3-L1	65.6 (2.4)	2.4 (0.29)	0.021	0.05 (0.01)	0.006 (0.001)	1.39×10^3	7.8 (0.05)
KA3-L2	56.9 (1.9)	12.1 (0.5)	0.43	5.2 (0.1)	0.46 (0.07)	24	11.2 (0.2)

Numbers in parentheses are the standard errors of curve fitting.
All k_{cat} and K_M measurements were conducted at pH 7.5, 25°C. Parameters were determined by non-linear least square fit of the Michaelis–Menten plots.
[a]Melting temperatures were determined by circular dichroism.

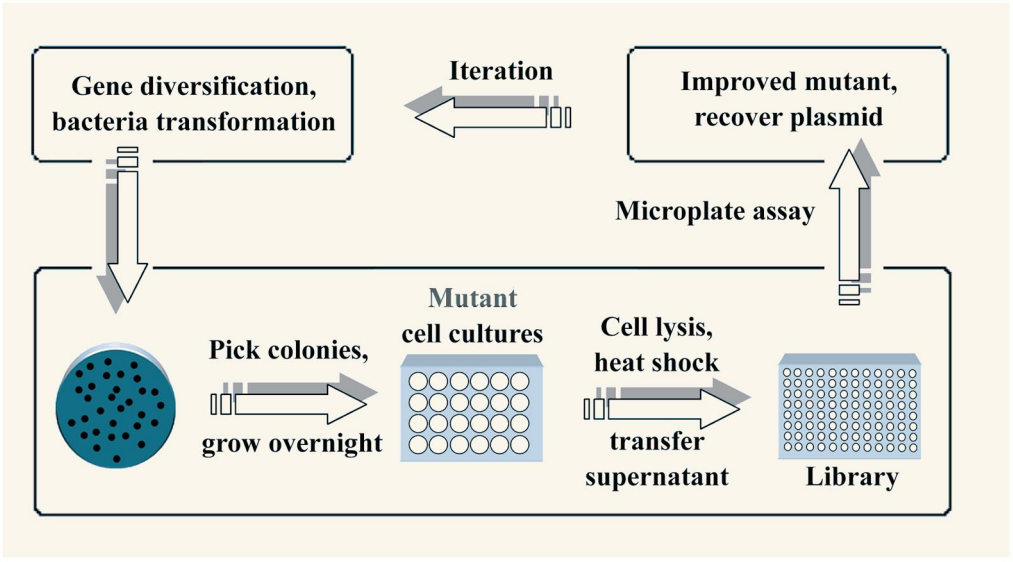

Figure 2. Schematic diagram showing the approach adopted for the directed evolution of KDPG aldolase.

adopted to evaluate the mutants generated in this study (Figure 2). KDG cleavage was monitored by a coupled enzyme assay, in which the pyruvate formed during the reaction was reduced to lactate by lactate dehydrogenase with concomitant oxidation of NADH to NAD. Assay samples were prepared on 96 well plates and the time-dependent decrease of NADH absorbance at 340 nm was monitored on a microtiter plate reader.

The 639 bp wild-type aldolase gene was amplified under standard mutagenic PCR conditions [17] with a controlled mutation rate of 2–3 bases per gene and then sub-cloned to an expression vector to generate the first generation plasmid library. The protein library was prepared by lysis of resuspended cell pellets harvested from 2 ml cultures of individually picked colonies obtained by transformation with the plasmid library.

Some unidentified background consumption of NADH was observed in our initial control experiments with cell lysate prepared in this manner. A noticeable baseline decrease at 340 nm was observed upon the addition of lactate dehydrogenase and NADH to the lysate but before the addition of the substrate. As the KDPG aldolase is comparatively stable with respect to thermal denaturation (Table 1), a heat treatment step was adopted for sample preparation to reduce the background consumption of NADH that may not be related to the aldol reaction. The lysed suspensions were heat treated at 65°C for 50 min to reduce background activity to zero and wild-type activity to a low but measurable level, and the supernatants were transferred to 96-well plates for screening assays at 25°C. About 30% of the first generation mutants still retained detectable activity after the heat treatment (Figure 3) but the baseline change before the addition of the substrate was no longer observable. An additional advantage of heat-shocking the

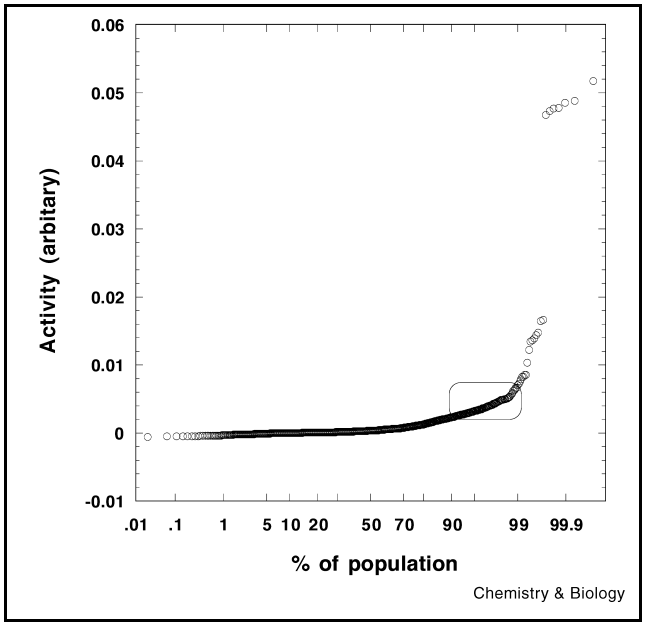

Figure 3. Statistics of relative enzyme activity obtained from the screening of the first generation library. Activity range of wild-type enzyme is indicated by a rectangle.

samples is that any mutant with improved activity selected from the pool must be either stable or relatively reversible with respect to thermal denaturation. Thus this study applies a stringent screening condition that exerts selective pressure on both activity at room temperature and thermal stability of the enzyme.

Of the 2400 first generation variants screened, 1% were more active than the wild-type enzyme for KDG cleavage. Amongst these, seven mutants (0.3% of the screened population) exhibited significant enhancement in the rate of KDG cleavage; 9% of the population retained activity comparable to the wild-type enzyme, and 90% were either not active or less active than the wild-type control (Figure 3). The high population of inactivated clones ($\sim$70%) could have resulted from the stringent heat treatment and a relatively low starting activity of the wild-type enzyme. A relatively high fraction of the first generation library exhibited beneficial mutations, suggesting that the wild-type enzyme is a good starting template for the evolution of activity under the thermal stability constraint.

Four genes of the selected first generation library that showed improvement in the cleavage of KDG (KA1-1, KA1-2, KA1-3 and KA1-4) were characterized, and then pooled and subjected to DNA shuffling [18] to produce the second generation library. 384 variants of this library were screened and two mutants (0.5% of the screened population) were identified with an improved rate. The best mutant (KA2) was selected and subjected to another cycle of mutagenic PCR and screening. 1024 variants of this resulting third generation library were screened and two improved mutants (0.2% of the screened population) were identified. Of these, the best third generation mutant KA3 was selected and analyzed.

Catalytic properties and thermal stability of evolved 'KDG' aldolases

The selected mutants were purified and analyzed for their ability to cleave KDPG and KDG. Progressive improvement of both k_{cat} and K_M was observed in the evolution of the aldolase towards KDG cleavage (Table 1). Compared with the wild-type enzyme, the third generation mutant KA3 has a 3-fold increase in k_{cat} and a 23-fold reduction in K_M, and hence a 70-fold improvement in catalytic efficiency (k_{cat}/K_M). The gain in the catalytic efficiency of KDG cleavage was accompanied by a decrease of KDPG cleavage. Interestingly, K_M for KDPG cleavage varied in parallel with that of KDG cleavage; however, the reduction in K_M for KDPG cleavage was offset by a large decrease in k_{cat} (110-fold) which caused the catalytic efficiency to decrease by 10-fold for the third generation mutant, compared with the wild-type. Thus, while the wild-type enzyme has remarkably high substrate specificity for KDPG over KDG ($[(k_{cat}/K_M)_{KDPG}/(k_{cat}/K_M)_{KDG}]_{WT} = 51\,000$), the evolved enzyme is much less specific for these substrates

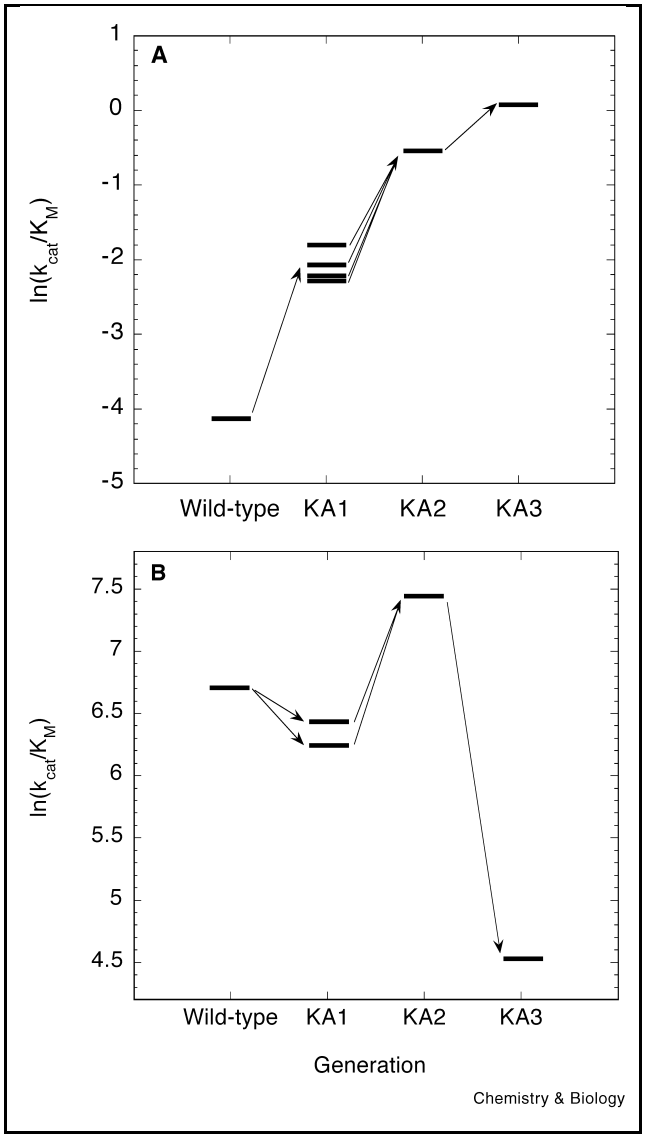

Figure 4. (A) Evolution of KDPG aldolase for KDG cleavage. **(B)** Effect of evolution towards KDG cleavage on KDPG cleavage. Only two of the first generation (KA1-2, KA1-3) mutants that are found to contribute to KA2 are shown.

($[(k_{cat}/K_M)_{KDPG}/(k_{cat}/K_M)_{KDG}]_{KA3} = 85$), and it corresponds to a 600-fold change in substrate specificity. These parameters suggest that the substrate binding site has been significantly altered in the evolved mutant. While the catalytic efficiency towards KDG cleavage is improved with successive cycles, the catalytic efficiency towards KDPG cleavage was altered unpredictably (Figure 4). The observed evolution pathway that reflects adaptation of the enzyme for reaction with a particular substrate (KDG) may exert an unpredictable effect on reactions with other substrates (KDPG) ("you get what you screen for" [2]). This behavior has been previously observed in another system [12].

Table 2
Relative activity of KDPG aldolase variants for aldol addition reactions with pyruvate as the donor substrate[a].

Acceptor substrate	Enzyme			
	Wild-type	KA3	KA3-L1	KA3-L2
D-Glyceraldehyde	100	181	32	165
L-Glyceraldehyde	[b]	26	23	30
D-Lactaldehyde	32	104	[b]	77
L-Lactaldehyde	–	–	–	–
DL-3-Fluoro-2-hydroxypropanal	45	95	27	91
D-Threose	–	–	–	–
D-Erythrose	–	–	–	–
DL-Glyceraldehyde-3-P	2.6×10^4	2.0×10^3	3.2×10^3	1.0×10^3
Glyoxylate	60	700	263	10
Glycolaldehyde	10	23	[b]	23
Chloroacetyldehyde	[b]	19	[b]	11

–, non-substrate.
[a]All assays were carried out with 50 mM aldehyde and 50 mM pyruvate. D-Glyceraldehyde and pyruvate concentrations are saturating for the wild-type enzyme [14]. Reactions were carried out at pH 7.5 and 30°C. The obtained reaction rates were normalized against the rate of the wild-type aldolase for D-glyceraldehyde addition.
[b]A reliable value could not be obtained because of slow reaction rate.

Wild-type KDPG aldolase catalyzes reversible aldol reactions between pyruvate and aldehyde substrates. Examination of KA3 to catalyze aldol addition reactions with pyruvate and several aldehydes reveals that except for glyceraldehyde 3-phosphate, the mutant has 2–10-fold improved activity compared with the wild-type (Table 2). Although the mutant is 10-fold less active in consuming phosphorylated glyceraldehyde, it is 10-fold more active towards glyoxylate. This suggests the change in activity may not be a result of a change in the electrostatic environment of the binding site.

Thermal denaturations of wild-type, KA1, KA2 and KA3 were monitored by circular dichroism, and a small change of the melting temperature was observed (Table 1). Aside from KA3-L2, which is slightly less stable than the wild-type (1.2°C), all other characterized mutants are slightly more stable than the wild-type. This suggests that the heat treatment procedure employed in sample preparation exerted a selective pressure on preserving the thermal stability of the enzyme. It is evident that mutations (Table 3) T84A and I92F act synergistically with V118A in improving both k_{cat} (2-fold) and K_M (2–3.5-fold) and thermal stability (6°C) of KA2. Such favorable combination of activity and thermal stability by mutation is very rare [11] and was not observed when the enzyme was evolved further.

Table 3
Mutations observed in KDPG aldolase variants obtained from screening.

Enzyme	Active mutations (amino acid)	Silent mutations (DNA)
KA1-4	E9K, V118A	C165T, T210C
KA1-3	V118A	–
KA1-2	T84A, I92F	A159G
KA1-1	G40A, V118A	C591T
KA2	T84A, I92F, V118A	A159G
KA3	T84A, I92F, V118A, E138V	A579G, A360G, A159G, C63T
KA3-L1	T84A, I92F, V118A, T161A	A159G
KA3-L2	T84A, I92F, V118A, G141S, T105I	C543T, A159G

Further screening for D-/L-glyceraldehyde selectivity

The wild-type enzyme is highly specific for aldehyde substrates with a D-configuration at C2 in the addition reaction. We examined the effect of mutations on the addition reactions between pyruvate and D- and L-glyceraldehyde respectively (Table 2). Compared with the wild-type aldolase, mutant KA3 exhibits a 1.8-fold and a considerable >5-fold improvement in rate for the addition of D-glyceraldehyde and L-glyceraldehyde respectively, to pyruvate at 50 mM substrate concentration. L-Glyceraldehyde has been reported to be a non-substrate for wild-type *E. coli* KDPG aldolase [14], but we found the wild-type enzyme accepts the aldehyde under the assay condition as a poor substrate. Enhancement in the addition rate of both D- and L-glyceraldehyde with pyruvate in the evolved mutant KA3 suggests that unlike KDPG, both D- and L-glyceraldehyde are good substrates for the evolved mutant.

Further screening of the library derived from KA2 for the consumption of L- and D-glyceraldehyde was attempted. After sampling 2000 variants and selecting for mutants that have a higher relative preference in accepting L-glyceraldehyde, KA3-L1 and KA3-L2 were identified (Table 2). Mutant KA3-L1 exhibited a significant loss of activity for D-glyceraldehyde compared with KA3; however, this was accompanied by an increase in activity with L-glyceraldehyde, to an extent comparable to KA3. By contrast, KA3-L2 displayed a 6-fold enhancement in activity with L-glyceraldehyde and a 1.6-fold enhancement in activity

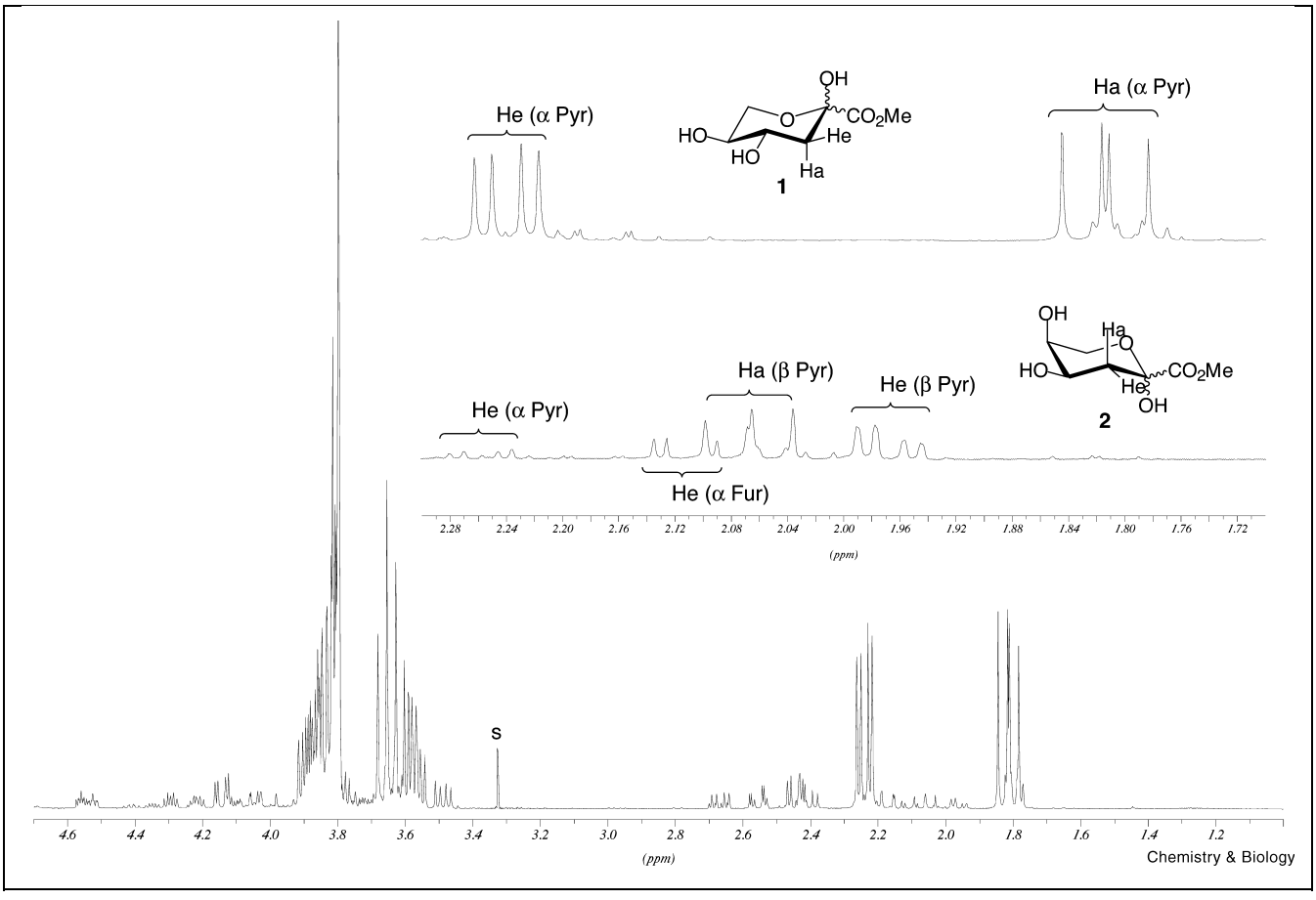

Figure 5. 1D NMR spectrum of a mixture of *threo* and *erythro* 3-deoxy-L-2-hexulosonic acid methyl ester in D_2O at room temperature. The mixture was prepared by KA3-L1 catalyzed addition of pyruvate to L-glyceraldehyde and then esterification. The inset shows the expanded regions for each of the isomer after chromatographic separation. Ratio of **1** to **2** was found to be 95.3:4.7 by integration of the peaks corresponding to the alpha protons.

with D-glyceraldehyde, compared with the wild-type. Thus, some mutations alter the enzyme activity on the two enantiomeric aldehydes independently. These preliminary results suggest the possibility of evolving mutants with a reversal of enantioselectivity, such that L-glyceraldehyde is a more favorable aldehyde substrate than D-glyceraldehyde. An extra stereo-center is formed during the addition of pyruvate to the acceptor aldehyde. To fully characterize the stereochemical property of the aldol adduct formed by the addition of pyruvate and L-glyceraldehyde, small preparative-scale addition reactions between L-glyceraldehyde and pyruvate catalyzed by KA3-L1 and KA3-L2 were carried out. The reactions yielded 3-deoxy-L-*threo*-2-hexulosonic acid (**1**) as the major product with ≥90% diastereomeric excess (Figure 5). Although measures were not taken to determine and control the facial selectivity of the addition reaction during this round of screening, the facial enantioselectivity was preserved in these two mutants.

With respect to the addition reactions of pyruvate to other aldehydes, mutant KA3-L2 behaves somewhat similarly to KA3 except with respect to the negatively charged glyoxylate and glyceraldehyde 3-phosphate. Whereas KA3-L1 has diminished activity towards other aldehydes, it exhibits enhanced activity towards the negatively charged glyoxylate and glyceraldehyde-3-phosphate compared with the wild-type.

Mutations observed in the evolved aldolases

Three of the four selected first generation mutants possess a common mutation, V118A (Table 3). Gene shuffling of these four mutated genes and screening eliminated E9K, G40A, and all existing silent mutations except A159G. The T84A, I92F and V118A mutations are favorable additive mutations that were recombined and preserved during the experiments. An additional favorable cumulative mutation E138V was introduced in the third round of mutagenesis and screening. These mutations appear to favor the bind-

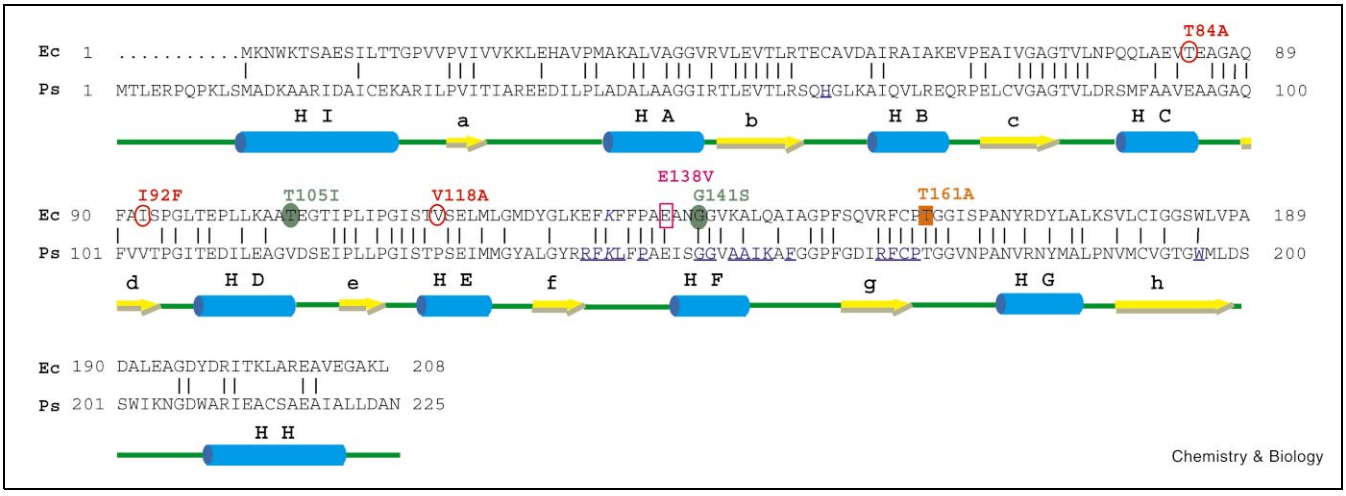

Figure 6. Sequence alignment of *P. putida* (Ps) and *E. coli* (Ec) KDPG aldolases. Putative active site residues are shown in blue and underlined and the Schiff base forming lysine (K144 of the *P. putida* sequence) is in italic and underlined. Schematic representation of the secondary structure elements of *P. putida* aldolase is shown underneath the sequences. α-Helices are represented as cyan cylinders, β-sheets as yellow arrows and loops as green bold lines. Common mutations found in mutants KA3, KA3-L1 and KA3-L2 (T84A, I92F, V118A) are marked with red empty ellipses, additional mutations found in KA3-L2 (T105I, G141S) are marked with green filled ellipses, in KA3-L1 (T161A) with a red filled box, and in KA3 (E138V) with a pink empty box.

Figure 7. Model of *E. coli* KDPG aldolase fragment 1–170 constructed based on homology to the known structure of *P. putida* aldolase, showing positions of mutations found in KA3, KA3-L1 and KA3-L2. Residues that were commonly mutated in KA3, KA3-L1 and KA3-L2 (T84, I92, V118) are in cyan, additional residues that were mutated in KA3-L2 (T105, G141) are in green, in KA3-L1 (T161) is in silver, and in KA3 (E138) is in pink. The putative Schiff base forming lysine (K133) is in gold. The model is displayed using InsightII 4.0 (Biosym). G141 is one of the residues that form the entrance of the active site. E138 is in the peripheral region of the active site. Other mutated residues do not seem to interact directly with the active site. Found mutations were located sufficiently far from each other. Direct interaction between the side chains of the mutated residues is not probable.

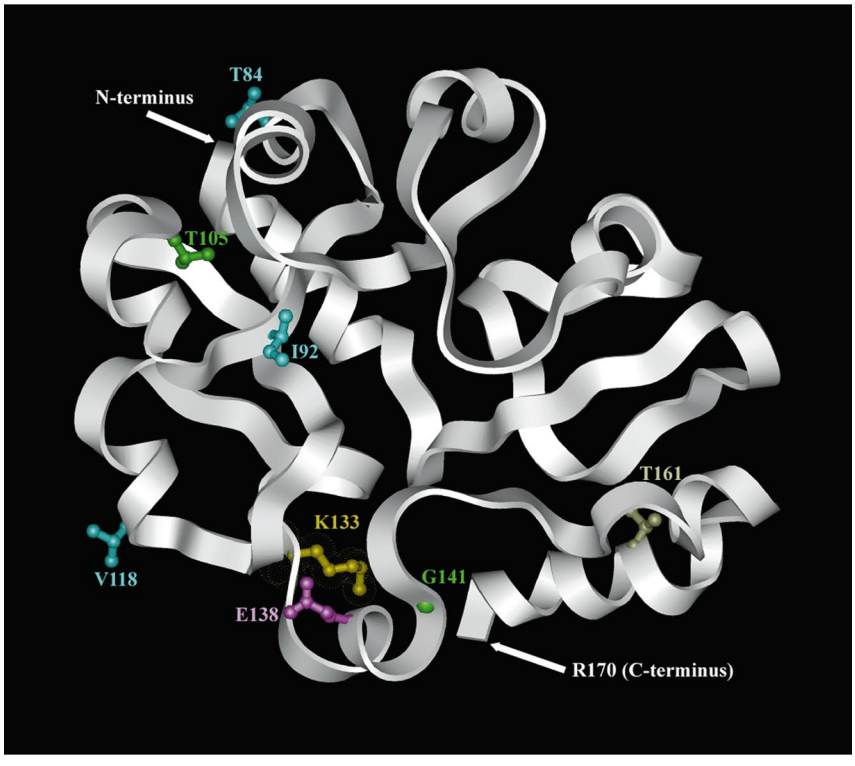

ing of KDPG, while they affect its cleavage turnover adversely.

To date, amongst the three most synthetically useful KDPG aldolases, crystallization and diffraction data collection were reported for the *E. coli* aldolase [19], although only the crystal structure of the *Pseudomonas putida* aldolase has been determined [20]. The *P. putida* enzyme belongs to the common TIM-barrel family and is believed to be trimeric in solution. Residues from different monomer units define the geometry of the active site and participate in binding and catalysis. The *E. coli* KDPG aldolase used in this study has substantial sequence homology with the *P. putida* enzyme [21], and exhibits 44% identical residues along with other conservative substitution patterns throughout the aligned sequences (Figure 6). The *E. coli* enzyme likely adapts the same fold as the *P. putida* enzyme with key catalytic residues arranged in a similar spatial orientation. According to the homology, a model of the *E. coli* enzyme was built (Figure 7). We speculate that T84A, I92F and V118A are not in close proximity to the enzyme active site. These mutations are located on regular secondary structure elements (helix-C, sheet-d and helix-E respectively) and the sequences at these sites are not completely conserved for the *P. putida* and *E. coli* proteins. E138 could be located in the peripheral region of the active site and this residue is in one of the conserved regions (132-F*K*FFPAE) which contains the proposed lysine Schiff base. Mutation E138V has opposite effects on the k_{cat} for the cleavage of the two substrates. This single mutation caused a 20-fold decrease in k_{cat} for KDPG cleavage but a 2-fold increase in k_{cat} for KDG cleavage. The mechanistic basis of this observation remains unclear. However, the residue could be important for proper substrate orientation during catalysis for the KA2 mutant. The observed mutations that alter the enzyme activity toward D- and L-glyceraldehyde may be located on helix-D (T105I), helix-F (G141S) and the beginning of the g-G loop (T161A). T161A is in the middle of a highly conserved region and this site is in the peripheral region of the active site. G141S is one of the sites that form the entrance of the active site cavity. Effects of mutations obtained from directed evolution experiments are often not obvious. For example, structural studies on *p*-nitrobenzyl esterase mutants reveals that mutations exert their influence over long distances. Reorganization of the enzyme active site was initiated by mutations elsewhere which orchestrate a series of main chain movement [22]. The advantage of the directed evolution approach is evident in this and other studies since desired enzyme properties can be achieved without prior structure–function knowledge. Furthermore, the causative effect and position of mutations observed are not readily predictable by rational design.

Significance

An efficient KDG aldolase has been evolved from *E. coli* KDPG aldolase. The evolved aldolase has very different catalytic efficiency and substrate specificity from the wild-type enzyme for the reversible aldol reaction. The viability of further evolution of the aldolase towards another trait (L-glyceraldehyde versus D-glyceraldehyde in the addition direction) has been demonstrated. By screening a small number (10^3) of mutants in successive libraries of low mutation rate (1 amino acid per 100 amino acids), it is feasible to improve progressively the activity of an enzyme by a significant amount towards a desired reaction with thermal stability as an additional stringency. Given a suitable screening method, the directed evolution approach can be a valuable general tool for rapid tuning of enzyme performance. With the recent advent of high throughput methods [23,24] for monitoring the extent of reactions, a practical screening strategy will be available to cover in principle the majority of enzymatic reactions in the near future. Work is in progress to develop a selection method to facilitate the evolution study and to alter the enzyme to exhibit a complete reversal of enantioselectivity.

Materials and methods

General procedures

Nucleic acid manipulations were done according to standard procedures [25]. Restriction endonucleases and T4 DNA ligase were purchased from New England Biolabs. *Taq* and *pfu* polymerases were purchased from Stratagene. UV kinetic assays were performed on a Cary 3 Bio UV-Vis spectrophotometer. NMR spectra (^{1}H, 400 MHz; ^{13}C, 100.6 MHz) were recorded on a Bruker AMX-400 spectrometer. ^{1}H NMR chemical shifts are referenced to residual protic solvent (D_2O $\delta_H = 4.80$). ^{13}C NMR chemical shifts are referenced to DMSO-d_6 ($\delta_C = 39.5$) as external standard. Mass spectra were recorded on a VG ZAB-ZSW mass spectrometer under fast atom bombardment or electrospray conditions. High resolution mass spectra were recorded on a IONSPEC FTMS (MALDI) with DHB as matrix. Circular dichroism and temperature denaturation was recorded on an AVIV model 62DS spectrometer. Temperature denaturation was monitored by ellipticity at 221 nm. Samples contained 2 μM protein and 10 mM of MOPS at pH 7.5. A temperature program with a heating rate of 1.2°C was used for all measurements. The apparent melting temperature was obtained by taking the derivative of the thermal denaturation data. The temperature at which the derivative reached the maximum was taken as the melting temperature. Optical rotations were measured with a Perkin-Elmer 241 polarimeter. All reactions were monitored by thin layer chromatography (TLC) performed on silica gel 60F_{254} precoated glass plates (EM Science), and compounds were visualized by charring after treatment with 5% w/v dodecamolybdophosphoric acid in water containing 10% H_2SO_4. Flash chromatography was carried out with silica gel 60 (230–400 mesh, EM Science). DNA sequencing was performed on an ABI50 automated sequencer. The reactions were performed using thermal cycle sequencing conditions with fluorescently labeled terminators. Curve fitting was done by the non-linear least squares method using KaleidaGraph (Abelbeck Software). Samples from 96 well plates were analyzed with a CERES UV900 Hdi reader (Bio-Tek instruments).

Plasmid construction

The 0.6 kb *E. coli* KDPG aldolase gene was amplified by standard PCR from a genomic preparation of *E. coli* JM109, with primers EdaTrc-F (5′-CAA TGC CAT GGA TAA AAA CTG GAA AAC AAG C) and EdaTrc-R (5′-AGC AGG TCG ACG GCG CTA TTC AGC TTA GCG CCC TCG AC) flanking the gene with restriction sites *Nco*I and *Sal*I. The resulting fragment was purified, doubly digested with *Nco*I and *Sal*I and ligated

into vector pTrcHis2A (Invitrogen) digested with the same restriction enzymes. The ligation product was transformed into *E. coli* XL1Blue-MRF′ by electroporation [26]. Plasmids recovered from transformants were screened by PCR for the presence of the aldolase insert. A positive plasmid clone *eda*-pTrcHis2A was sequenced, used for protein expression and as mutation template for the construction of the first generation library.

Mutagenic PCR was carried out under standard error-prone conditions [17]. Primers EdaTrc-F and EdaTrc-R were used to amplify and mutate the template gene. 40 pmol of each of the primers was used and the reaction conditions were: 10 ng template/10 mM Tris–HCl, pH 8.3/50 mM KCl/1.5 mM $MgCl_2$/0.5 μl DMSO/0.2 mM $MnCl_2$/0.2 mM each of dATP, dTTP, dCTP, dGTP/2.5 U *Taq* polymerase (Stratagene), in a total volume of 50 μl. The mixture was thermocycled for 30 rounds of 94°C, 1 min; 55°C, 1 min; 72°C 1 min, and then one round of 72°C for 30 min. The library fragment was gel purified and cloned into pTrcHis2A as described above and the resulting library construct was transformed into XL1Blue-MRF′, amplified and purified as plasmid miniprep (Qiagen). The presence of the gene insert in the library constructs was confirmed by gel electrophoresis with the parent vector pTrcHis2A as reference. Heterogeneity of the first generation library construct was examined by transforming the plasmid into JM109 followed by random picking of 13 colonies, plasmid extraction, and DNA sequencing. The selected clones contained the following mutation(s): C195T (Pro65Leu), T511C (silent)/T402C (Phe134Ser), C595T (silent)/A100G (silent), T519A (Leu173Gln)/C521T (Ala174Val), G532A (Val178Met)/C34A (Leu12Met), A273T (silent), A431T (Lys144Ile)/A289G (Thr97Ala), T395A (Phe132Tyr)/A134G (Glu45Gly), T287C (Leu96Pro)/T248C (Val83Gly), G297A (silent), G483A (silent)/C331T (silent)/C56A (Pro19Gln), T131A (L44Gln), A101G (Lys34Arg), T268C (Phe90Leu)/C281A (Pro94Gln), G606T (Lys202Asn)/T332C (Leu111Pro), A380G (Tyr127Cys), C477T (silent)/no mutation.

DNA shuffling was done according to the method of Stemmer [18]. Fragments of 50–100 bp were isolated and used for the reassemble PCR. Substrate for shuffling was prepared by standard PCR of a mixture of the four selected plasmids from the first generation library. A thermal cycling program of 94°C for 60 s; 94°C for 30 s, 55°C for 30 s, 72°C for 30 s (35 cycles); and 72°C for 1 min was used for the reassemble PCR and the amplification of the reassembled product.

Library screening for KDG cleavage

Constructs harboring the mutant library were transformed into JM109 by electroporation. Transformed culture was spread on Luria–Bertani (LB) agar plates containing 50 μg/ml of ampicillin and incubated at 37°C for 16 h. Individual colonies were picked, replicated on a LB agar-ampicillin plate, and dispensed into 24-well plates containing in each well 2 ml of LB with 50 μg/ml ampicillin and 0.2 mM IPTG (the broth was shaken vigorously before dispensing into the plates). The plates were sealed and shaken at 37°C and 200 rpm in a shaker-incubator for 18 h, centrifuged at 4000 rpm and 4°C for 1 h, and the supernatant was carefully decanted. Each cell pellet was resuspended in 0.5 ml of 50 mM potassium phosphate buffer, pH 7.5 containing 0.5 mg/ml of lysozyme. The plates were rapidly frozen in liquid nitrogen followed by thawing at room temperature, and then incubated at 65°C for 50 min. Cell debris was pelleted by centrifugation at 4000 rpm, 4°C for 1 h. 0.2 ml of supernatant from each well was transferred to a separate well on a 96-well plate. Upon incubation at 25°C for at least 10 min, 25 μl of assay solution containing 50 mM potassium phosphate, NADH and L-lactic dehydrogenase at pH 7.5 was dispensed into each well with an 8-channel-repeating pipette. In each well, the starting concentration of NADH was 705 μM, and 5 U of lactic dehydrogenase was present. Baseline drift at 340 nm was monitored for 2 min. All samples had leveled or insignificant baseline drift. 25 μl of KDG at 18 mg/ml (10 mM starting concentration) in 50 mM potassium phosphate, pH 7.5 was added to each well and the absorbance at 340 nm was monitored at 20 s intervals continuously for 5 min after an initial 10 s of medium strength shaking. Activity of each mutant was reflected by the rate of decrease of OD_{340nm}. Mutants that had unusually high activity were selected. The selected mutant colonies were picked from the replicated LB agar-ampicillin plate, grown overnight in LB-ampicillin medium, and their plasmids extracted as DNA minipreps (Qiagen) and sequenced.

Library screening for D- and L-glyceraldehyde utilization

Samples for assay on the 96-well format were prepared as described above. Each sample was duplicated in pair, and one was assayed for D-glyceraldehyde and the other for L-glyceraldehyde. Upon incubation at 25°C for at least 10 min, 25 μl of assay solution containing potassium phosphate (50 mM), pyruvate and glyceraldehyde at pH 7.5 was added to each well. The starting concentrations for pyruvate and glyceraldehyde in each well were 2 mM and 11 mM respectively. Upon incubation at 25°C, 25 μl of NADH was added to each well to a concentration of 705 μM with an 8-channel-repeating pipette, and the baseline at 340 nm was recorded for 5 min. 5 U of lactic dehydrogenase was added to each well with an 8-channel-repeating pipette and the absorbance at 340 nm was monitored for 5 min at 20 s intervals. The baselines after the burst phase upon the addition of lactic dehydrogenase were extrapolated to the zero time point to obtain the *y*-intercepts. The differences between the *y*-intercepts obtained before and after the addition of lactic dehydrogenase were used to estimate the amount of pyruvate remaining in each sample. Plates containing D-glyceraldehyde were incubated for 10 min prior to the assay whereas plates containing L-glyceraldehyde were incubated for 30 min prior to the assay, to allow the addition reactions to occur.

Enzyme expression and purification

Selected plasmids were transformed into JM109. To express the protein, starter culture was prepared by picking individual colony and inoculated into 5 ml of LB-ampicillin medium, at 37°C, 220 rpm overnight. The starter culture was added to 500 ml of LB-ampicillin medium, and was incubated at 37°C, 220 rpm. Protein expression was induced at $OD_{600nm} = 0.4$, by the addition of IPTG to a final concentration of 0.2 mM. Cells were harvested 6 h after the induction, by centrifugation at 4°C, 8000 rpm for 10 min and were stored at −78°C. The cell pellet from 500 ml culture was resuspended in 20 ml of 50 mM potassium phosphate pH 7.5/5 mM β-mercaptoethanol/300 mM NaCl, chilled on ice, and was lysed by passing through a French press (SLM Instruments, Urbana, IL) compressed to 1500 psi and then released to ambient pressure. The process was repeated three times. Cell debris was pelleted by centrifugation at $12\,000 \times g$, 4°C for 1 h. The supernatant was filtered through a 0.2 μm cellular acetate membrane filter (Corning), and was loaded onto a Ni^{2+}-NTA-agarose column with a bed volume of 2.5 ml pre-equilibrated with the cell resuspension buffer. The column was washed with 40 ml of buffer containing 50 mM potassium phosphate pH 7.5/5 mM β-mercaptoethanol/300 mM NaCl/5% glycerol/10 mM imidazole, and then 40 ml of buffer containing 50 mM potassium phosphate pH 7.5/5 mM β-mercaptoethanol. Bound enzyme was eluted with 50 mM potassium phosphate pH 7.5/5 mM β-mercaptoethanol/250 mM imidazole, and was dialyzed extensively against 50 mM potassium phosphate pH 7.5/5 mM β-mercaptoethanol at 4°C. Eluted enzymes were analyzed with SDS–PAGE and were found to be $>90\%$ pure in all cases. Enzyme solution was frozen in liquid nitrogen and was stored at −78°C prior to use. No activity loss was observed upon freezing and thawing the enzymes. Enzyme concentrations were determined by the Bradford procedure (Bio-Rad) using bovine serum albumin as a calibration standard.

KDPG/KDG cleavage assay

Activity was determined by the standard coupled assay with L-lactic dehydrogenase (EC 1.1.1.27, type II from rabbit muscle) and NADH. A typical assay was initiated by the addition of an appropriate amount of KDG or KDPG in 50 mM potassium phosphate, pH 7.5/5 mM β-mer-

captoethanol, to a mixture of L-lactic dehydrogenase (10 U)/NADH (0.43 mM)/aldolase (0.88 μM) in 50 mM potassium phosphate, pH 7.5/5 mM β-mercaptoethanol. The total reaction volume was 800 μl. Prior to the addition of the substrate, the mixture was preincubated at 25°C for 5 min. UV absorbance at 340 nm was recorded continuously for 2 min and the slope of the absorbance curve during the first 30 s was used for rate determination.

Assay for addition reaction

Activity was determined by the rate of depletion of pyruvate. Pyruvate concentration was determined by a method similar to that previously reported [14]. Reactions were initiated by the addition of the aldolase to a mixture of pyruvate and glyceraldehyde preincubated at 30°C. Reactions were performed in 2 ml volume. Starting concentrations of pyruvate, glyceraldehyde and enzyme were 50 mM, 50 mM and 2 μM, respectively. 25 μl aliquots were withdrawn from the reaction mixture at different time points and quenched with 30 μl of 7% perchloric acid. Samples were neutralized with 20 μl of 1 M NaOH. 15 μl of each neutralized sample was diluted to 800 μl and assayed for pyruvate.

Preparation of D-2-keto-3-D-deoxygluconate (KDG)

A mixture of 25 ml of 1 M sodium gluconate in 50 mM Tris–HCl pH 8.0 and 30 ml of crude D-gluconate dehydratase from 0.5 l culture of *Alcaligenes faecalis* (ATCC 9220), prepared according to the method of Kersters [27], was stirred at ambient temperature for 16 h. Formation of KDG was detected by TLC eluted with methanol:ethyl acetate 1.5:1 and stained with a modified procedure of the thiobarbituric acid assay [28]. Proteins in the reaction mixture were precipitated by the addition of 25 ml of 70% perchloric acid and pelleted by centrifugation at 4°C/8000 rpm for 20 min. The supernatant was neutralized with 10 N KOH and the precipitate formed was removed by suction filtration. The solution was diluted to 100 ml with distilled water and was loaded to an AG-1X8-formate column prewashed with 1 M sodium formate and then distilled water. The column was eluted with a linear gradient of 0–1 M formic acid, the product containing fractions were pooled and solvent was removed in vacuo. The residue was stripped with water in vacuo several times to removal residual formic acid and was dried to yield 2.9 g (65%) of KDG as white solid. ^{1}H NMR is identical to that reported in the literature [29] and no signal due to the diastereomeric product could be observed. ESIMS: *m/e* 201 $(M+Na)^+$, 177 $(M-H)^-$.

Preparation of D-2-keto-3-deoxy-6-phosphogluconate (KDPG)

KDPG was prepared following the method of O'Connell and Meloche [30].

Preparation of 3-deoxy-threo-2-hexulosonic acid methyl ester

Sodium pyruvate (50 mg, 0.45 mmol), L-glyceraldehyde (45 mg, 0.499 mmol) and KA3-L1 (4 mg, 0.038 mol%) in 2.5 ml of 50 mM phosphate buffer at pH 7.5 containing 5 mM β-mercaptoethanol was incubated at 37°C for 2 days. The pH of the mixture was adjusted to 2 by adding 7% perchloric acid, and the precipitate was removed by centrifugation. The supernatant was diluted to 10 ml and applied to an AG-1X8-formate column prewashed with 1 M sodium formate and then distilled water. The column was eluted with a linear gradient of 0–1 M formic acid, product containing fractions were pooled and solvent was removed in vacuo. The residue was stripped with water in vacuo several times to remove residual formic acid and dried to yield 12.8 mg (16%) of colorless liquid. ^{1}H NMR is complex but is consistent with the signals attributed from one major product (*threo*) and one minor product (*erythro*). The product mixture was taken up in anhydrous methanol (1.5 ml) and methanol washed and dried Dowex 50W-X4 (H^+, 2 mg) was added. The resulting mixture was stirred at ambient temperature for 10 h and the resin filtered. The filtrate was concentrated and the residue first purified by flash chromatography (CH_2Cl_2/MeOH, 10/1) followed by a second chromatography (EtOAc/EtOH, 50/1) to afford 0.9 mg of *erythro* methyl ester and 11.5 mg of *threo* methyl ester as colorless oils.

The same reaction was carried out with sodium pyruvate (50 mg, 0.45 mmol), L-glyceraldehyde (45 mg, 0.499 mmol) and KA3-L2 (4 mg, 0.038 mol%) in 2.5 ml of 50 mM phosphate buffer at pH 7.5 containing 5 mM β-mercaptoethanol. The mixture was incubated at ambient temperature for 5 days and 42 mg (52%) of colorless liquid was obtained upon the ion exchange column step as described. Esterification and chromatography of the aldol adducts yielded 2.7 mg of *erythro* and 34.5 mg of *threo* methyl esters as colorless oils.

Spectral data for the *erythro* isomer: $[\alpha]_D^{20}$ +14.1 (*c* 0.27 in $CHCl_3$, lit. $[\alpha]_D^{28}$ −14 for 2-keto-3-D-deoxygluconate methyl ester in $CHCl_3$); HRMS (MALDI), calcd. for MNa^+ $C_7H_{12}O_6Na$ *m/e* 215.0526, found *m/e* 215.0532. The ^{1}H and ^{13}C NMR data are the same as those for the enantiomer reported previously [29]. Spectral data for the *threo* isomer: $[\alpha]_D^{20}$ −10.3 (*c* 1.4 in MeOH); HRMS (MALDI), calcd. for MNa^+ $C_7H_{12}O_6Na$ *m/e* 215.0526, found *m/e* 215.0519. The ^{1}H and ^{13}C NMR data of the predominant form (α-pyranose) in D_2O are the same as those reported previously [31].

Preparation of DL-3-fluoro-2-hydroxypropanal

The compound was prepared following the method reported by Durrwachter et al. [34].

Modeling of E. coli KDPG aldolase

The only available molecular coordinates of the *P. putida* KDPG aldolase (Protein Data Bank reference 1KGA) contain only the Cα trace for the 9–181 fragment of the enzyme. The missing backbone and side chain coordinates for this fragment were predicted and generated with MaxSprout [32]. The resulting structure was used as an input template for homology modelling with Modeller 4 [33] using standard procedures. Fragment 1–170 of the *E. coli* aldolase was aligned with fragment 9–181 of the *P. putida* aldolase as shown in Figure 6 and was used as the input alignment file.

Acknowledgements

This research was supported by the NIH GM44154. The authors would like to thank Drs. Thomas Tolbert, Grace DeSantis and Pamela Sears for helpful discussions.

References

1. Machajewski, T.D. & Wong, C.-H. (2000). The catalytic asymmetric aldol reaction. *Angew. Chem. Int. Ed. Engl.* **39**, 1352–1374.
2. Arnold, F.H. (1998). Design by directed evolution. *Acc. Chem. Res.* **31**, 125–131.
3. Altamirano, M.M., Blackburn, J.M., Aguayo, C. & Fersht, A.R. (2000). Directed evolution of new catalytic activity using the α/β-barrel scaffold. *Nature* **403**, 617–622.
4. Takato, Y., Shinya, O. & Hiroyuki, K. (1998). Directed evolution of an aspartate aminotransferase with new substrate specificities. *Proc. Natl. Acad. Sci. USA* **95**, 5511–5515.
5. Zhang, J.-H., Dawes, G. & Stemmer, W.P.C. (1997). Directed evolution of a fucosidase from a galactosidase by DNA shuffling and screening. *Proc. Natl. Acad. Sci. USA* **94**, 4504–4509.
6. Stemmer, W.P.C. (1994). Rapid evolution of a protein in vitro by DNA shuffling. *Nature* **370**, 389–391.
7. MacBeath, G., Kast, P. & Hilvert, D. (1998). Redesigning enzymatic topology by directed evolution. *Science* **279**, 1958–1961.
8. Reetz, M.T., Zonta, A., Schimossek, K., Liebeton, K. & Jaeger, K.-E. (1997). Creation of enantioselective biocatalysts for organic chemistry by in vitro evolution. *Angew. Chem. Int. Ed. Engl.* **36**, 2830–2832.
9. May, O., Nguyen, P.T. & Arnold, F.H. (2000). Inverting enantioselectivity by directed evolution of hydantoinase for improved production of L-methionine. *Nature Biotechnol.* **18**, 317–320.
10. Zhao, H. & Arnold, F.H. (1999). Directed evolution converts subtilisin E into a functional equivalent of thermitase. *Protein Eng.* **12**, 47–53.
11. Giver, L., Gershenson, A., Freskgard, P.-O. & Arnold, F.H. (1998).

Directed evolution of a thermostable esterase. *Proc. Natl. Acad. Sci. USA* **95**, 12809–12813.
12. Moore, J.C. & Arnold, F.H. (1996). Directed evolution of a para-nitrobenzyl esterase for aqueous-organic solvents. *Nature Biotechnol.* **14**, 458–467.
13. You, L. & Arnold, F.H. (1994). Directed evolution of subtilisin E in *Bacillus subtilis* to enhance total activity in acqueous dimethylformamide. *Protein Eng.* **9**, 77–83.
14. Shelton, M.C., Cotterill, I.C., Novak, S.T.A., Poonawala, R.M., Sudarshan, S. & Toone, E.J. (1996). 2-Keto-3-deoxy-6-phosphogluconate aldolases as catalysts for stereocontrolled carbon-carbon bond formation. *J. Am. Chem. Soc.* **118**, 2117–2125.
15. Peekhaus, N. & Conway, T. (1998). What's for dinner?: Enter-Doudoroff metabolism in *Escherichia coli*. *J. Bacteriol.* **180**, 3495–3502.
16. Cotterill, I.C., Shelton, M.C., Machemer, D.E.W., Henderson, D.P. & Toone, E.J. (1998). Effect of phosphorylation on the reaction rate of unnatural electrophiles with 2-keto-3-deoxy-6-phosphogluconate aldolase. *J. Chem. Soc. Perkin Trans.* **1**, 1335–1341.
17. Leung, D.W., Chen, E. & Goeddel, D.V. (1989). *Technique* **1**, 11–15.
18. Stemmer, W.P.C. (1994). DNA shuffling by random fragmentation and reassembly: In vitro recombination for molecular evolution. *Proc. Natl. Acad. Sci. USA* **91**, 10747–10751.
19. Buchanan, L.V., Mehta, N., Pocivavsek, L., Niranjanakumari, S., Toone, E.J. & Naismith, J.H. (1999). Initiating a structural study of 2-keto-3-deoxy-6-phosphogluconate aldolase from *Escherichia coli*. *Acta Crystallogr. D Biol. Crystallogr.* **D55**, 1946–1948.
20. Mavridis, I.M., Hatada, M.H., Tulinsky, A. & Lebioda, L. (1982). Structure of 2-keto-3-deoxy-6-phosphogluconate aldolase at 2.8 Å resolution. *J. Mol. Biol.* **162**, 419–444.
21. Egan, S.E., Fliege, R., Tong, S., Shibata, A., Wolf, R.E.J. & Conway, T. (1992). Molecular characterization of the Entner-Doudoroff pathway in *Escherichia coli*: Sequence analysis and localization of promoters for the edd-eda operon. *J. Bacteriol.* **174**, 4638–4646.
22. Spiller, B., Gershenson, A. & Arnold, F.H. (1999). A structural view of evolutionary divergence. *Proc. Natl. Acad. Sci. USA* **96**, 12305–12310.
23. Reetz, M.T., Becker, M.H., Klein, H.-W. & Stockigt, D. (1999). A method for high-throughput screening of enantioselective catalysts. *Angew. Chem. Int. Ed. Engl.* **38**, 1758–1761.
24. Reetz, M.T., Becker, M.H., Kuhling, K.M. & Holzwarth, A. (1998). Time-resolved IR-thermographic detection and screening of enantioselectivity in catalytic reactions. *Angew. Chem. Int. Ed. Engl.* **37**, 2647–2650.
25. Sambrook, J., Fritsch, E.F. & Maniatis, T. (1989). *Molecular Cloning: A Laboratory Manual*. (2nd edn), Cold Spring Harbor Laboratory Press, Plainview, NY.
26. Dower, W.J., Miller, J.F. & Ragsdale, W. (1988). High efficiency transformation of *E. coli* by high voltage electroporation. *Nucleic Acids Res.* **16**, 6127–6145.
27. Kersters, K. & De Ley, J. (1975). D-Gluconate dehydratase from *Alcaligenes*. *Methods Enzymol.* **42**, 301–304.
28. Warren, L. (1960). Thiobarbituric acid spray reagent for deoxy sugars and sialic acids. *Nature* **186**, 237.
29. Plantier-Royon, R., Cardona, F., Anker, D., Condemine, G., Nasser, W. & Robert-Baudouy, J. (1991). Nouvelle synthèse de l'acide 3-désoxy-D-erythro-2-hexulosonique (KDG). A partir de la D-glucono-1,5-lactone synthèse et étude de rmn de dérivés o-méthyles du KDG. *J. Carbohydr. Chem.* **10**, 787–811.
30. O'Connell, E.L. & Meloche, H.P. (1982). Enzymic synthesis of 2-keto-3-deoxygluconate 6-phosphate using 6-phosphogluconate dehydratase. *Methods Enzymol.* **89**, 89–101.
31. Alessi, F., Doutheau, A. & Anker, D. (1996). Synthesis of methyl esters of 3-deoxy-D-*erythro*-2-hexulosonic acid (KDG) analogs, inducers of the expression of pectinase genes in bacteria *Erwinia chrysanthemi*. *Tetrahedron* **52**, 4625–4636.
32. Holm, L. & Sander, C. (1991). Database algorithm for generating protein backbone and side-chain coordinates from a Cα trace application to model building and detection of coordinate errors. *J. Mol. Biol.* **218**, 183–194.
33. Sali, A. & Blundell, T.L. (1993). Comparative protein modelling by satisfaction of spatial restraints. *J. Mol. Biol.* **234**, 779–815.
34. Durrwachter, J.R., Drueckhammer, D.G., Nozaki, K., Sweers, H.M. & Wong, C.-H. (1986). Enzymatic aldol condensation/isomerization as a route to unusual sugar derivatives. *J. Am. Chem. Soc.* **108**, 7812–7818.